



AMERICAN METEOROLOGICAL SOCIETY

Journal of Applied Meteorology and Climatology

EARLY ONLINE RELEASE

This is a preliminary PDF of the author-produced manuscript that has been peer-reviewed and accepted for publication. Since it is being posted so soon after acceptance, it has not yet been copyedited, formatted, or processed by AMS Publications. This preliminary version of the manuscript may be downloaded, distributed, and cited, but please be aware that there will be visual differences and possibly some content differences between this version and the final published version.

The DOI for this manuscript is doi: 10.1175/JAMC-D-16-0271.1

The final published version of this manuscript will replace the preliminary version at the above DOI once it is available.

If you would like to cite this EOR in a separate work, please use the following full citation:

Bates, B., A. Dowdy, and R. Chandler, 2017: Classification of Australian Thunderstorms using Multivariate Analyses of Large-Scale Atmospheric Variables. *J. Appl. Meteor. Climatol.* doi:10.1175/JAMC-D-16-0271.1, in press.

© 2017 American Meteorological Society



1 **Classification of Australian Thunderstorms using Multivariate Analyses of Large-Scale**
2 **Atmospheric Variables**

3
4 BRYSON C. BATES

5 *CSIRO Oceans and Atmosphere, Wembley, Western Australia, Australia*

6 *School of Earth and Environment, The University of Western Australia, Crawley, Western*
7 *Australia, Australia*

8
9 ANDREW J. DOWDY*

10 *Bureau of Meteorology, Melbourne, Victoria, Australia*

11
12 RICHARD E. CHANDLER

13 *Department of Statistical Science, University College London, London, UK*

14
15 ABSTRACT

16 Lightning accompanied by inconsequential rainfall (i.e. 'dry' lightning) is the primary
17 natural ignition source for wildfires globally. This paper presents a machine-learning and
18 statistical-classification analysis of 'dry' and 'wet' thunderstorm days in relation to
19 associated atmospheric conditions. The study is based on daily lightning flash count and
20 precipitation data from ground-based sensors and gauges, and a comprehensive set of
21 atmospheric variables based on the ERA-Interim reanalysis for the period from 2004 to 2013
22 at six locations in Australia. These locations represent a wide range of climatic zones
23 (temperate, subtropical to tropical). Quadratic surface representations and low-dimensional
24 summary statistics were used to characterize the main features of the atmospheric fields. Four
25 prediction skill scores were considered and ten-fold cross validation used to evaluate the

*Corresponding author (Email: andrew.dowdy@bom.gov.au; Tel: + 61 3 9669 4722)

26 performance of each classifier. The results were compared with those obtained by adopting
27 the approach used in an earlier study for the Pacific Northwest, United States. It was found
28 that: both approaches have prediction skill when tested against independent data, mean
29 atmospheric field quantities proved to be the most influential variables in determining dry
30 lightning activity and no single classifier or set of atmospheric variables proved to be
31 consistently superior to their counterparts for the six sites examined here.

32

33 **1. Introduction**

34 Although human-caused wildfire ignitions are common in many regions of the world,
35 particularly in densely populated areas, fires ignited by lightning typically burn a larger area
36 than fires ignited by other sources. This is attributable to lightning occurrence in remote
37 locations and in large spatial and temporal clusters which hamper the response efforts of fire
38 management authorities (USDA Forest Service 1992; McRae 1992; Vazquez and Moreno
39 1998; Wotton et al. 2005; Wotton and Martell 2005; Kasischke et al. 2006; Dowdy and Mills
40 2012a). Lightning that occurs with relatively little precipitation (i.e., ‘dry’ lightning) has a
41 higher chance of igniting a fire than lightning accompanied by heavier precipitation (‘wet’
42 lightning) (Rothermel, 1972; Wotton and Martell 2005; Dowdy and Mills 2012a). Therefore,
43 an improved understanding of dry lightning activity and the atmospheric conditions that
44 influence its occurrence is of importance for better preparedness and enhancing the ability to
45 respond to the impacts associated with wildfires ignited by lightning.

46 There are many physical factors that can influence lightning occurrence as demonstrated
47 in numerous previous climatological, dynamical modeling and seasonal prediction studies
48 including Weisman and Klemp (1982), Goodman et al. (2000), Burrows et al. (2005),
49 Williams et al. (2005), Deierling et al. (2008), Romero et al. (2007), Chronis et al. (2008),
50 Dai et al. (2009), Barthe et al. (2010), Romps et al. (2014), Magi (2015), Dowdy (2016),

51 Muñoz et al. (2016) and references therein. Although aspects of the microphysical processes
52 associated with lightning generation are not well understood in some cases, the role of ice in
53 facilitating charge separation within the cloud appears to be a critical factor in determining
54 whether or not lightning is produced (e.g., as indicated by laboratory experiments (Takahashi
55 and Miyawaki 2002) as well as observations (Lang et al. 2014)). Microphysical processes
56 such as ice formation are not well represented at the spatial and temporal scales of currently
57 available climate models and reanalyses, leading to the use of parameterization schemes for a
58 range of variables associated with convection. For example, the ERA-Interim reanalysis (Dee
59 et al. 2011) uses a convective parameterization based on a bulk mass flux scheme (as
60 originally described by Tiedtke 1989), with parameterizations also used to represent the
61 fallout of precipitation (e.g., Kuo and Raymond 1980) and factors such as virga (streaks of
62 water or ice particles that vaporize before reaching the ground) considered.

63 In addition to convective parameterization schemes, several studies have demonstrated
64 that statistical indicators of lightning activity can be found at relatively coarse spatial and
65 temporal scales (e.g., similar to the resolution of general circulation models (GCMs) and
66 reanalyses). For example, Romps et al. (2014) combined precipitation and Convective
67 Available Potential Energy (CAPE) based on GCM output for use as an indicator of
68 environments conducive to lightning activity, applying this indicator to examine the influence
69 of global warming on lightning strikes in the United States. A recent study based on
70 reanalyses demonstrated that even at spatial resolutions of 7.5° in latitude and longitude,
71 atmospheric conditions such as lower-tropospheric moisture content, temperature lapse rate
72 and CAPE can be strongly related to lightning activity (Dowdy 2016).

73 In contrast to the number of studies that have examined atmospheric conditions associated
74 with lightning activity in general, relatively few studies have focused specifically on dry
75 lightning. Notable early studies include Rorig and Ferguson (1999, hereafter designated as

76 RF99) and Rorig et al. (2007), demonstrating that a linear discriminant rule could separate
77 dry and wet lightning classes. The rule was composed of dewpoint depression at 850 hPa
78 (DD850) and temperature lapse from 850 to 500 hPa (TL850500), with dry lightning defined
79 as lightning accompanied by precipitation of less than one tenth of an inch (about 2.5 mm).
80 Dowdy and Mills (2012b) demonstrated that these two variables were also applicable in
81 southeast Australia, and that the average chance of a sustained fire ignition resulting from the
82 occurrence of lightning in that region is higher than average if the precipitation
83 accompanying the lightning is less than about 2 to 3 mm. Recent studies have examined a
84 somewhat wider range of variables in relation to the occurrence of dry lightning, including
85 studies in North America (Wallmann et al. 2010; Nauslar et al. 2013; Abatzoglou et al. 2016)
86 and Australia (Dowdy 2015), finding that some useful skill can be obtained for predicting the
87 occurrence of dry lightning based on several different methods. However, as dry lightning
88 activity remains relatively unstudied when compared with other aspects of thunderstorm
89 activity and associated convective processes, to date there have been no climatological
90 studies of the spatial and temporal variability of dry lightning activity, or the influence of
91 large-scale atmospheric drivers of dry lightning variability.

92 The approach presented in this paper (hereafter designated as BDC) represents a more
93 general approach to the two-category classification problem of dry and wet lightning days
94 than that of RF99. The paper has four objectives with a view to building on previous studies
95 of dry lightning occurrence. The first is to consider a wider range of atmospheric conditions
96 associated with dry lightning activity and precipitation occurrence than has been the case to
97 date. The second is to build on the suggestion put forward by Blouin et al. (2016) that a
98 comparison of classification methods (classifiers) may provide useful guidance for future
99 research. The third is to consider lightning, precipitation and atmospheric data from a wide
100 range of climatic zones. The fourth objective is to identify a subset of influential atmospheric

101 variables across climatic zones and different classifiers. The method of RF99 is used as a
102 benchmark for assessments of prediction accuracy and the applicability of the new approach
103 proposed in this paper. In this way, the paper provides a useful addition to the toolkit for
104 addressing questions related to lightning activity. The paper is divided into five sections.
105 Section 2 provides a description of the study sites, data and classifiers used. Results are
106 presented in Section 3. A summary and conclusions are given in Section 4. The quadratic
107 surface representations and low-dimensional summary statistics (LDSS) used to characterize
108 the main features of the atmospheric fields considered in this study are described in the
109 Appendix.

110

111 **2. Data and methods**

112 *a. Description of study sites and data*

113 The description of the daily lightning flash count datasets used herein parallels that of
114 Bates et al. (2015), and the text in the next two paragraphs is derived from there with minor
115 modifications. The data were collected from ground-based CIGRE 500 (Comité
116 Internationale des Grands Réseaux Electriques, 500 Hz peak transmission filter circuit)
117 sensors located at six weather stations operated by the Australian Bureau of Meteorology
118 (Figure 1 and Table 1). The sensors were selected because of their record length and quality,
119 and their locations in a variety of climatic settings including temperate, subtropical and
120 tropical sites. The records cover the period from January 2004 to at least December 2010
121 (Townsville) and at most February 2013 (Melbourne).

122

123 **< Insert Figure 1 and Table 1 about here >**

124

125 Although the CIGRE 500 sensor was designed specifically to detect cloud-to-ground
126 flashes, it also responded to cloud-to-cloud flashes, with about 68% of the lightning flash
127 counts recorded being due to cloud-to-ground flashes. We considered the total number of
128 lightning flash counts since the CIGRE 500 sensor did not distinguish between intracloud and
129 cloud-to ground flash counts; and the ratio of intracloud to cloud-to-ground flashes can vary
130 significantly depending on thunderstorm type and intensity, region of occurrence and season
131 (Rakov and Uman, 2003). Estimates of the effective horizontal ranges of the sensor are 30
132 km for cloud-to-ground flashes and 15 km for cloud-to-cloud flashes (Kuleshov and
133 Jayaratne, 2004). As with other studies of this nature, these effective ranges should be taken
134 into consideration when interpreting results for specific purposes such as fire ignition from
135 cloud-to-ground lightning flashes. The electromechanical counters attached to the CIGRE
136 500 sensors were read manually each day between 0800 and 0900 h local time. Further
137 details can be found in Jayaratne and Kuleshov (2006), Kuleshov et al. (2009) and Bates et al.
138 (2015).

139 For a given weather station, thunderstorms were deemed to have occurred during a 24-h
140 period if at least one lightning flash count was registered by the CIGRE 500 sensor. They
141 were categorized as either 'dry' or 'wet' according to the concurrent daily precipitation
142 reading recorded by the storage gauge at the station. A thunderstorm was classified as dry if
143 the precipitation reading was less than 2.5 mm or wet otherwise. In Australia, daily
144 precipitation is nominally measured each day at 0900 h local time. Station data were obtained
145 from the SILO patch-point data set (Australian Bureau of Meteorology). There is a large
146 disparity in spatial scales between the detection range of the sensor and the diameter of a
147 precipitation gauge (15-30 km versus 203 mm). Thus it is possible for precipitation amounts
148 greater than 2.5 mm to occur within the sensor's detection limit but away from the station
149 gauge. However, the use of gridded station data has its own set of limitations in that the

150 interpolation involved is a form of smoothing that reduces precipitation variability. Thus, the
151 process of gridding can considerably increase (decrease) the frequency of low (high)
152 precipitation amounts (Ensor and Robeson, 2008), and this might have implications for the
153 classification of dry thunderstorms. The reduction in variability is dependent on the distance
154 from a grid point to the nearest gauge. A further concern is the relatively low density of
155 precipitation gauge networks in Australia. For example, the numbers of gauges within a 30
156 km radius of the Darwin, Townsville, Coffs Harbour and Port Hedland sites are 12, 8, 18 and
157 3, respectively. This low network density is likely to lead to excessive smoothing in some
158 instances and affect the distribution of daily precipitation amounts. Given the above, days
159 with station precipitation values flagged as interpolated were discarded.

160 With future applications in mind, the study was designed to be conducted at spatial and
161 temporal resolutions similar to that of current general circulation models and reanalyses.
162 Atmospheric information was obtained from the ERA-Interim reanalysis archive (Dee et al.
163 2011). The spatial and temporal resolution of the dataset used is 0.75 degrees (in both latitude
164 and longitude) and 6 hours, respectively. For each CIGRE 500 site, atmospheric data were
165 extracted for the 49 reanalysis grid points closest to the sensor's location. The aim of the grid
166 was to capture the presence of a thunderstorm over or in the proximity of a sensor. The
167 lightning and precipitation series were synchronized with the ERA-Interim series for 0600
168 UTC (1600 h Eastern Australia Time) within the 24-hour period represented by the lightning
169 and precipitation data. This is because the diurnal variation in temperature lapse rate over
170 land, due to solar radiation, produces conditions that are more favorable for lightning activity
171 to occur during the late-afternoon period in general than at other times of the day or night
172 (Christian et al. 2003; Dowdy and Mills 2009; Allen et al. 2011). Thus, the synchronization
173 ensures that the atmospheric variables for each daily lightning flash count correspond to the
174 time at which the lightning is most likely to have occurred. Since the use of a single time

175 point can be viewed as reductive, the possibility that atmospheric variables at other times of
176 day may also be relevant was considered. However, the additional information was found to
177 be largely redundant because correlations within a 24-hour period are invariably high (e.g.
178 correlations between individual variables at 0600 UTC and 1200 UTC, spanning the time
179 period during which most deep convective processes occur in Australia, are typically greater
180 than 0.95 and greater than 0.85 in every case examined). The atmospheric variables
181 considered herein are listed in Table 2.

182

183 **< Insert Table 2 about here >**

184

185 The set of atmospheric variables examined here represents a wider range than has typically
186 been examined in previous studies, particularly those studies focused on climate-scale
187 analyses rather than finer-resolution numerical weather prediction or radar observational
188 studies. This is because there have been very few studies that have specifically examined dry
189 lightning activity and the atmospheric conditions that influence its occurrence. Consequently,
190 the literature on dry and general lightning activity was combed and physical understanding
191 used to reduce the number of variables as far as possible. The variables listed in Table 2
192 represent a broad variety of physical processes that can be associated with deep convection,
193 including both dynamical and thermodynamical processes. The variables comprise various
194 measures of temperature lapse, moisture content, vertical motion and water phase state,
195 including at a range of different pressure levels (to allow potential variations in height
196 between dry and wet thunderstorm characteristics to be distinguished).

197 *b. Variable selection*

198 To identify the dominant large-scale controls on lightning activity from among the
199 variables listed in Table 2 is a challenging statistical problem: there are dependencies among

200 the variables leading to collinearity and, moreover, the processes controlling lightning
201 activity are complex so that the variables must be considered concurrently rather than in
202 isolation. Regression-based approaches, notably those based on generalized linear models,
203 are ideally suited to this kind of problem (e.g. Yan et al. 2002, Chandler 2005). However, an
204 additional complication in the present application is that the explanatory variables are spatial
205 fields over a 7×7 grid, rather than individual values. In principle, this can be handled using
206 modern statistical techniques such as functional regression (e.g. Morris, 2015). However, in
207 their current state of development such methods are most effective when the number of
208 candidate variables is relatively small. The current state of knowledge is insufficient to
209 identify a small number of candidate variables from the list in Table 2 with high confidence.
210 The strategy adopted here is therefore to use a combination of approaches that are designed to
211 isolate the most influential variables from many candidates.

212 To handle the spatial nature of the atmospheric variables listed in Table 2, the daily fields
213 for each variable were reduced to a set of five LDSS designed to capture the main synoptic
214 features. This was done by fitting quadratic surfaces to each daily field (see Appendix) and
215 using the fitted surfaces to derive physically-interpretable daily summaries (overall means,
216 vertical and horizontal gradients, and curvature). Note that the intention is not to provide
217 highly accurate descriptions of the fields, but rather to provide indices that broadly describe
218 the synoptic structure. The use of LDSS reduces the dimensionality of the problem from 49
219 grid point values per atmospheric variable per day to 5. Other dimension reduction techniques
220 are available, notably principal component (empirical orthogonal) analysis which was
221 explored as an alternative to the LDSS considered here. It was found that five or more
222 components were necessary to explain 70 to 80% of the variance for each data set. Only the
223 first component had any predictive power in terms of discriminating between dry and wet
224 lightning. Although the loadings for this component would often indicate a contrast between

225 two sets of variables, a defensible interpretation of the contrast proved elusive. Moreover, its
226 predictive skill was lower than that obtained with LDSS.

227 At this point, a LDSS of an atmospheric variable will be referred to as a potential
228 candidate variable. As an initial screening procedure, for each potential candidate variable,
229 comparative boxplots of each LDSS were used to contrast its values for dry and wet lightning
230 cases. Two variable selection criteria were considered. First, potential candidate variables
231 where the 75th (25th) percentile for one lightning type was below (above) the 25th (75th)
232 percentile for the other were deemed informative in terms of discriminating between dry and
233 wet lightning days. These variables were reserved for further analysis. Second, depending on
234 the number of such candidate variables found, they were supplemented by including
235 additional candidate variables where the median in one lightning type was above the 75th
236 percentile or below the 25th percentile of the other (see, e.g., Figure 2). The resulting
237 candidate variables formed the columns of an atmospheric data matrix. This approach could
238 be criticized as ad hoc: it is natural to ask whether alternative techniques, such as automatic
239 variable selection procedures, would be preferable. The main reason for the approach taken
240 here is that manual inspection of boxplots can provide checks on the data, as well as
241 preliminary insights that may aid subsequent interpretation and that cannot be obtained from
242 an automated analysis. In any case, the aim is merely to carry out a very preliminary
243 screening of the data so as to focus subsequently on quantities that may have some predictive
244 power in discriminating between dry and wet lightning.

245

246 < **Insert Figure 2 about here** >

247

248 Many of the candidate variables are measured on very different scales and thus are not
249 commensurable in terms of magnitude or variability. This means that some variables could

250 dominate or influence the results of the classification analysis because of their measurement
251 units alone (Everitt and Hothorn, 2011). Thus, the columns of the data matrix were
252 standardized to zero mean and unit variance prior to further analysis. This process places
253 candidate variables on the same relative scale without disturbing the shape of the distribution
254 of the data. It facilitates interpretation of the results of a discriminant or regression analysis,
255 and helps to concentrate precisely on the conditions that are present during thunderstorms
256 because it focuses on the relative variations of each variable within its own physical limits.
257 The `colldiag` function from the `perturb` package in the R computing environment (Hendrickx
258 2012; R Core Team 2015) was used to detect the presence of collinearity in the data matrix.
259 `Colldiag` is an implementation of the regression collinearity diagnostic procedures found in
260 Belsley et al. (1980). It computes the condition indices of the data matrix and provides the
261 variance decomposition proportions associated with each condition index. As a rule of thumb,
262 variables with proportions greater than 0.99 were considered sources of severe collinearity.
263 Thus the corresponding columns were removed to form a reduced data matrix. A second
264 proportion threshold of 0.8 was used to assess the degree of the sensitivity to threshold
265 selection. It was found that the results obtained from the procedures described below showed
266 only a slight sensitivity. Therefore, the results obtained using the proportion threshold of 0.8
267 will not be reported here.

268 *c. Multivariate statistical analysis*

269 Two machine-learning and three statistical methods were used for classification:
270 classification and regression trees (CART); random forests (RF); linear discriminant analysis
271 (LDA), quadratic discriminant analysis (QDA) and logistic regression (LR). Detailed
272 descriptions of CART, RF and LR can be found in Faraway (2016), and LDA and QDA in
273 Everitt and Dunn (2001). The R packages used in this work were: `DiscriMiner` (Sanchez
274 2013); `MASS` (Venables and Ripley, 2002); `randomForest` (Liaw and Wiener 2002); and `tree`

275 (Ripley, 2014). CART uses binary recursive partitioning to divide the data space, splitting it
276 along the coordinate axes of the candidate variables to give increasingly homogenous subsets
277 and hence the maximal separation of the classes until it is infeasible to continue. The measure
278 of node heterogeneity is the deviance (a quality-of-fit statistic). The partitioning leads to a set
279 of decision rules in the form of a binary tree. The tree is ‘pruned’ to identify a parsimonious
280 tree with acceptable misclassification rates. Cross validation can be used to determine an
281 appropriate tree size. RF is an ensemble learning algorithm which generates a large number
282 of CART from bootstrap samples of the original data. An estimate of the misclassification
283 rate can be obtained by using each tree to predict the data not in the bootstrap sample and
284 averaging the predictions over all trees. The randomForest package can be used to produce
285 variable importance plots which reveal how important each variable is in classifying the data
286 and contributing to the homogeneity of the nodes. LDA is derived from an underlying model
287 in which the distributions of the variables on dry and wet lightning days are both multivariate
288 normal, with possibly different means and a common covariance matrix. LDA is somewhat
289 robust with respect to minor violations of these assumptions. Although serious violations will
290 often result in unreliable estimates of the coefficients, the procedure can still be a good
291 heuristic. The discriminant function is a linear combination of the candidate variables, the
292 coefficients of which are estimated by ordinary least squares so that the ratio of the between-
293 classes variance and the within-classes variance is maximized. This function takes the value
294 zero at the decision boundary. If the value of the discriminant function is negative the
295 variable vector is assigned to one class, if positive it is assigned to the other class. Given that
296 the variables are standardized, the coefficients indicate the relative importance of each
297 variable in predicting class assignment. QDA is a generalization of LDA in which the two
298 classes need not have the same covariance matrix, but the assumption of multivariate
299 normality still applies. The interpretation of the coefficients in terms of the relative

300 importance of each variable is more difficult to assess than for LDA as the discriminant
 301 function contains quadratic as well as linear and constant terms. The LR model can be written
 302 as

$$304 \quad \text{logit}(\pi_i) = \ln[\pi_i/(1-\pi_i)] = \beta_0 + \sum_{j=1}^p \beta_j X_j \quad (1)$$

305
 306 where π_i is the probability of occurrence of class i ($i = 1, 2$), $\pi_i/(1-\pi_i)$ is the odds ratio for
 307 class i , p is the number of columns in the data matrix and β_0, \dots, β_p are the regression
 308 coefficients which are determined via maximum likelihood estimation. (Obviously, with only
 309 two categories it is only necessary to estimate the coefficients for one of the categories since
 310 $\pi_2 = 1 - \pi_1$.) Classification on the basis of the variables is then done by setting a threshold τ
 311 say, and allocating a day to category 1 if $\pi_1 > \tau$. For each site, a receiver operating
 312 characteristic (ROC) curve was used to select the threshold τ by minimizing the distance
 313 from the curve to the point representing perfect classification accuracy: this was done to
 314 account for the fact that the sample sizes for dry and wet lightning days were noticeably
 315 unequal for several sites (Table 1). Experiments using Youden's (1950) Index indicated that
 316 threshold estimates were not sensitive to the selection technique used. With LR, by contrast
 317 with LDA and QDA, there is no formal requirement for multivariate normality of the
 318 explanatory variables within each category of the response variable, and the use of binary or
 319 categorical variables is acceptable. A combination of stepwise selection and analysis of
 320 deviance was used to determine the significance of variables in the LR models. Further
 321 details on the above classifiers can be found in Breiman (2001), Venables and Ripley (2002)
 322 and Hilbe (2009).

323 Although the approach of RF99 used only LDA to discriminate between dry and wet
324 lightning, the four other classifiers considered herein (CART, RF, QDA and LR) were
325 applied to the means of the DD850 and TL850500 fields (designated μ .DD850 and
326 μ .TL850500, see Appendix) to ascertain whether a higher classification performance could
327 be achieved. This extended approach is hereafter designated as E-RF99. The analysis was
328 conducted in parallel with an identical study of a much larger set of variables to determine the
329 extent to which it is possible to improve on the RF99 variable pair. Four measures of
330 prediction skill were considered: the hit rate for dry lightning (HR), the false alarm ratio for
331 dry lightning (FAR), the Brier (1950) score (BS) and for LR the area under the ROC (AUC).
332 HRs, FARs, BSs, ROC curves and AUCs were determined using the verification package in
333 R (NCAR 2015). For a perfect classification, HR=1, FAR=0, BS=0 and AUC=1. HR values
334 near 0, FAR and BS values near 1, and AUC values near 0.5 indicate poor classification
335 performance. For the convenience of the reader, in what follows, a list of the acronyms and
336 abbreviations used in this paper and their meaning is given in Table 3.

337

338 **< Insert Table 3 about here >**

339

340 *d. Cross validation experiments*

341 Initial assessments of the prediction skill of the five classifiers (CART, RF, LDA, QDA
342 and LR) were based on the data matrices for the six CIGRE 500 sites. As this can lead to
343 optimistic bias in the estimated skill scores, ten-fold cross validation experiments were used
344 to assess how well the results generalized to an independent dataset. Here the lightning,
345 precipitation and candidate variable data were partitioned into ten subsamples of equal size.
346 From these subsamples, a single subsample was retained for testing the model, and the
347 remaining nine subsamples used for training (model fitting). The process is then repeated ten

348 times with each of the subsamples used exactly once for validation. The R packages used in
349 the cross validation experiments were cvTools (Alfons 2012) and verification (NCAR 2015).

350

351 **3. Results**

352 *a. Preliminary analyses*

353 Lightning activity at the six sites occurs primarily during the warmer months of the year
354 (November to April). However, the most severe fire weather conditions in Australia occur at
355 different times of the year, generally ranging from summer in the south to winter (i.e., the dry
356 season) in the north. There are some regional variations to this, particularly along the eastern
357 seaboard (including Coffs Harbour) where the peak fire weather conditions occur somewhat
358 earlier (around October) than at other similar latitudes in Australia (Luke and McArthur,
359 1978). Further details on the lightning climatology of Australia may be found in Kuleshov et
360 al. (2009), Dowdy and Kuleshov (2014), Bates et al. (2015) and references therein, and will
361 not be repeated here.

362 The proportions of dry and wet lightning days for the six CIGRE 500 sites are reported in
363 Table 1 and illustrated in Figure 1. Darwin is one of the most lightning prone areas in
364 Australia. The number of lightning days for Darwin is markedly higher than those for the
365 remaining sites, even for the case of Townsville which is in the same climatic zone. Perth has
366 the lowest number of lightning days by a wide margin. Port Hedland has the highest
367 proportion of dry lightning days, reflecting its desert environment. For the tropical and
368 subtropical sites, the proportion of dry lightning days exceeds that of wet lightning days. This
369 is somewhat surprising, and may in part be explained by the use of a single precipitation
370 gauge to characterize rainfall over the detection range of the CIGRE 500 sensor (Section 2).
371 To a lesser extent, it might reflect the effects of the precipitation threshold of 2.5 mm on

372 lightning day classification. For example, the proportions of dry and wet lightning days at
373 Darwin are essentially equal if the precipitation threshold is reset to 2.0 mm.

374 Median adjusted R^2 values for the fitted quadratic surfaces varied from variable to variable
375 with 5.2 to 16% below 0.5 across the six CIGRE 500 sites and 47 to 68% above 0.75. The
376 highest values were obtained for GPH500 and GPH700 (> 0.97), and the lowest for W and
377 MING, (0.09 to 0.43). This pattern was consistent across all sites. Thus, overall, the quadratic
378 surfaces described in the Appendix gave a reasonable representation of the main features of
379 the atmospheric fields considered herein.

380 *b. Classification analyses*

381 Scatterplots of the skill scores obtained from the five classifiers are shown in Figure 3.
382 The HR and FAR are for dry lightning and the radii of the circles represent the magnitude of
383 the BS. For each CIGRE 500 site, the convex hull of the five data points obtained using only
384 mu.DD850 and mu.TL850500 as candidate variables is displayed to facilitate their
385 delineation. (The convex hull of a set of points is the smallest convex set enclosing the
386 points.) The plots reveal six key features. First, for any site, approach (E-RF99 or BDC) and
387 classifier, the HR exceeds the FAR (note the differences in the axis scales). Thus, both
388 approaches and all five classifiers have some skill in discriminating dry lightning from wet
389 lightning. Apart from Port Hedland, it is also evident that the RF99 approach (denoted by
390 filled squares enclosed by green circles) provides lower HRs. Second, for Darwin and
391 Townsville the approach of BDC often provides higher HRs than those for E-RF99 but at
392 expense of higher FARs for some classifiers. Third, for Coffs Harbour, Melbourne and Perth,
393 the approach of BDC produced simultaneously higher hit rates and lower FARs than those for
394 E-RF99. Fourth, in the case of Port Hedland, the HRs and FARs obtained for a given
395 classifier and the two approaches considered herein (E-RF99 and BDC) are similar despite
396 the differences in candidate variable sets: the BDC candidate variable set included terms such

397 as μ .TOTP, μ .CONVP and μ .TCW (see Appendix for details regarding their derivation).
398 Fifth, except for Darwin, the application of LR to the BDC candidate variable set produced
399 low FARs. Sixth, the approach of BDC produces similar or lower BSs than those for E-RF99.

400

401

< Insert Figure 3 about here >

402

403

c. Influential variables

404 The relative frequency histogram of influential variables across the six CIGRE 500 sites
405 and four classifiers with easily interpreted decision rules or boundaries (CART, RF, LDA and
406 LR) is shown in Figure 4. Overall, 16 out the 28 variables are means, nine are magnitudes of
407 gradient vectors, two are vertical gradients and one is SEASON (Table 2). The seven most
408 frequent variables are associated with atmospheric water content (μ .TOTP, μ .CONVP,
409 gd .TOTP and μ .TCWV) and instability and lifting potential (μ .CBH, μ .DD700 and
410 vg .T). Thus, five of the seven most frequent variables are means. In terms of the raw
411 atmospheric variables listed in Table 2, not one of the variables used by RF99 (DD850 and
412 TL850500) is present in this subset. Additionally, DD850 does not appear to be as influential
413 as DD700, with DD700 and DD850 having relative frequencies of 0.0879 and 0.0220. As
414 shown in Fig. 2c, high values of DD700 are typically associated with dry lightning rather
415 than wet lightning, with a physical interpretation of this being that relatively dry air results in
416 an increased likelihood of precipitation evaporating before reaching the ground (i.e., virga).
417 The absence of CAPE and the near absence of W in Figure 4 suggest that these variables are
418 not informative in terms of discriminating between dry and wet lightning conditions. This is
419 unlikely to be the case for lightning activity studies involving discrimination between
420 lightning and non-lightning days.

421 The dominance of the mean terms in the set of influential variables could be related to
422 temporal variations in the timing of thunderstorms with respect to a given location, noting
423 that although our analyses is based on afternoon values of the atmospheric variables (as this
424 is when lightning most frequently occurs in these regions), lightning can also occur at other
425 times of the day and night. The apparent influence of $\mu.TOTP$ and $\mu.CONVP$ must give
426 rise to concern that information about precipitation has been used twice: once as daily
427 precipitation readings at ground-based storage gauges were used to classify lightning days as
428 either dry or wet; and twice as $\mu.TOTP$ and $\mu.CONVP$ values at 0600 UTC were derived
429 from modeled precipitation and used as explanatory variables. However, scatter plots and
430 quantile-quantile plots of $\mu.TOTP$ and $\mu.CONVP$ against the precipitation readings (not
431 shown) revealed little evidence of relationships for all six CIGRE 500 sites. Except for
432 Melbourne, robust estimates of the correlation coefficients ranged from 0.1 to 0.3. For
433 Melbourne, the estimates were about 0.4. This lack of a simple relationship, and the positions
434 of $\mu.TOTP$ and $\mu.CONVP$ in the histogram depicted in Figure 4, suggest that the
435 construction of these variables captures useful additional information about atmospheric
436 conditions that cannot be obtained from the other potential candidate variables considered.
437 Some evidence for this conjecture is provided in Davies et al. (2013). For one of the tropical
438 sites considered herein (Darwin), they created two concurrent long-term data sets that
439 described the large-scale atmosphere and the characteristics of small-scale convection. They
440 found that estimates of convective precipitation have a strong relationship with dynamical
441 variables such as moisture convergence and vertical velocity at mid-levels. Wind rather than
442 moisture convergence was used in the current study (Table 2), and vertical velocities in
443 reanalyses can suffer from large inaccuracies (Abalos et al., 2015). The latter may have also
444 contributed to the position of $\mu.W$ and $gd.W$ in Figure 4.

445

446 < Insert Figure 4 about here >

447

448 Figure 5 displays the relative frequency histograms of the most-frequent atmospheric
449 variables on a site-by-site basis. Here the maximum frequency for any variable is limited to
450 four (the number of classifiers with interpretable decision rules or boundaries). Furthermore,
451 the minimum count for any variable can be zero as not every one of the variables was found
452 to be influential for every site. Colored bars indicate the seven most-frequent variables
453 depicted in Figure 4. For the sake of clarity, white bars indicate additional variables that have
454 a frequency of at least two. The variables depicted in Figure 5 are primarily associated with
455 atmospheric water content and instability and lifting potential. Comparison of Figures 5a-d
456 and 5e-f indicates a marked difference in the shapes of the histograms for sites located in
457 western Australia (Perth and Port Hedland) and those in central and eastern Australia
458 (Darwin, Townsville, Coffs Harbour and Melbourne). In the case of Perth (Figure 5e), five of
459 the seven most-influential variables across all sites and classifiers depicted in Figure 4 have
460 zero frequencies and the frequencies of the remaining two (μ .CBH and gd .TOTP) are low.
461 It is the only site not to include both μ .TOTP and μ .CONVP amongst its set of influential
462 variables. The most common variables across the four classifiers for Perth are indicated by
463 white bars. Three of these four variables (μ .TGM7001000, gd .GPH500 and gd .GPH700)
464 are not included in the variable sets for the other sites (cf. Figure 4). These variables are
465 potential indicators of convective systems associated with fronts. The fourth variable
466 (μ .TL850500) is selected for Coffs Harbour by LR only. For Port Hedland (Figure 5f),
467 three of the seven most frequent variables in Figure 4 have zero frequencies. It is the only site
468 to not include μ .CBM amongst its set of influential variables. The remaining four variables
469 (μ .TOTP, μ .CONVP, gd .TOTP and m .TCWV) characterize atmospheric water content.
470 There are four additional variables (gd .TOTP, gd .CONVP, μ .MING and μ .T2) that are

471 not depicted in Figure 5f since they have a frequency of one. Port Hedland is also different to
472 the other sites in that it has a notably higher HRs and lower FARs (Figure 3). This is because
473 the ratio of dry to wet lightning proportions for Port Hedland is 4.3 which is much higher
474 than that for the other sites where it is between 1.1 and 1.8 (Table 1). With the exceptions of
475 Townsville and Coffs Harbour, the frequencies of $vg.T$ are zero for the four remaining sites.
476 Sharp temperature gradients are a potential indicator of troughs, and convergence along
477 troughs can lead to showers and thunderstorms. The so-called inland (or easterly) trough is
478 located on the inland side of the Great Dividing Range in Australia, forming a boundary
479 between the moist air near the coast and dry air inland. It typically extends through central
480 Queensland and into central New South Wales and is active during the months from
481 September to May. Furthermore, the frequency of $mu.ICE$ is greater than zero for Melbourne
482 alone. Ice water content and lightning activity are highly correlated (Xu et al., 2010 and
483 references therein), and this variable may provide information about the low (high) lightning
484 flash rates associated with dry (wet) lightning. These results, and those illustrated in Figure 4,
485 suggest that the optimal variable sets for lightning classification problems may vary between
486 different climatic zones.

487

488 **< Insert Figure 5 about here >**

489

490 *d. Cross validation experiments*

491 Scatterplots of the mean skill scores obtained from the cross validation experiments are
492 shown in Figure 6. Again, the HR and FAR are for dry lightning and the radii of the circles
493 represent the magnitude of the BS. The radii of the circles have been placed on the same scale
494 as those shown in Figure 3. The plots in Figure 6 reveal five key features. First, in all cases
495 the mean HR exceeds the mean FAR. This indicates that both approaches (E-RF99 and BDC)

496 and the classifiers considered herein have prediction skill when tested with independent data.
497 While this is also true for the approach of RF99, the mean HRs are relatively low compared
498 to those of either the E-RF99 or BDC approach. Second, the plots confirm the earlier finding
499 that the approach of BDC generally provides either higher hit rates, or simultaneously higher
500 hit rates and lower FARs, than that of E-RF99. Third, the mean FARs obtained using QDA
501 are not always robust. This is particularly evident for Townsville, Melbourne, Perth and Port
502 Hedland. This reflects the method's sensitivity to outliers. Fourth, when tested with
503 independent data, applying LR to the BDC variable set often produced the lowest or
504 competitive mean FARs. Fifth, the approach of BDC often produces competitive or lower
505 BSs when tested with independent data than that of E-RF99.

506

507 **< Insert Figure 6 about here >**

508

509 A scatterplot of AUC values obtained from cross-validation of the LR models is shown in
510 Figure 7. For all sites and both approaches (E-RF99 and BDC), the AUC values are greater
511 than 0.5 indicating that prediction skill is better than climatology. However, the AUCs for the
512 BDC approach are greater than those for E-RF99. The lowest AUC values were obtained for
513 Darwin and the highest for Port Hedland (E-RF99 approach) and Perth (BDC approach).

514

515 **< Insert Figure 7 about here >**

516

517 **4. Summary and conclusions**

518 Daily lightning flash count and precipitation data from ground-based sensors and gauges,
519 atmospheric information from the ERA-Interim reanalysis and five classification techniques
520 (classifiers) were used to distinguish between 'dry' and 'wet' thunderstorm days for the

521 period from 2004 to 2013 at six locations in Australia. The locations of the lightning flash
522 (CIGRE 500) sensors represent a range of climatic settings (including temperate, subtropical
523 and tropical regions). The earlier approach of Rorig and Ferguson (1999, RF99), which used
524 two atmospheric variables and one classifier (linear discriminant analysis) for one region in
525 the United States (the Pacific Northwest), was used as a benchmark to test whether the
526 inclusion of additional atmospheric information and a wider range of classifiers resulted in a
527 notable improvement in prediction accuracy for the climatic settings considered herein.

528 With future applications in mind, the study was designed to be conducted at the spatial
529 resolution of current GCMs and reanalyses. Quadratic surfaces and determination of low-
530 dimensional summary statistics (LDSS) were used to capture the main features of the
531 atmospheric fields. Five classifiers were considered: classification and regression trees
532 (CART); random forests (RF); linear discriminant analysis (LDA), quadratic discriminant
533 analysis (QDA) and logistic regression (LR). Four prediction skill scores were considered,
534 with a focus on dry lightning since it is the primary cause of wildfire ignition. Ten-fold cross
535 validation was used to estimate the prediction accuracy of the classifiers. The study findings
536 can be summarized as follows:

- 537 1) The use of LDSS captured useful and interpretable information in terms of the large-scale
538 spatial structure of thunderstorms. While it can be argued that the LDSS are somewhat
539 crude, our results suggest that there is value in their application to the problem of
540 thunderstorm classification.
- 541 2) The approach outlined in this paper (BDC) and an extended version of that of Rorig and
542 Ferguson (1999, herein designated as E-RF99) have prediction skill when tested against
543 independent data for a wide range of climatic zones.
- 544 3) Overall, while five LDSS were used to better capture the main features of the atmospheric
545 fields used, the mean field proved to be the most useful. The seven most-frequent

546 variables across the six sites and five classifiers considered are associated with
547 atmospheric water content (μ .TOTP, μ .CONVP, gd .TOTP and μ .TCWV) and
548 instability and lifting potential (μ .CBH, μ .DD700, and vg .T). The preceding lists of
549 variables contain five spatial means, two gradient terms and variables derived from
550 convective parameterizations. The results presented herein suggest that the latter may
551 provide unique information that is not contained in ground-based precipitation data.

552 4) Despite the finding above, the set of influential atmospheric variables varied from site-to-
553 site and between classifiers. This result needs to be tested using data from dense
554 monitoring networks in different countries and a wide variety of climatic zones. The
555 question of whether it is legitimate to use the same atmospheric variables and statistical
556 classification techniques at different locations within the same climatic zone will be the
557 subject of future research.

558 5) No single classifier proved to be consistently superior to its counterparts across the six
559 sites considered. However, LR often produced lower FARs while the predictive accuracy
560 of QDA was compromised by the presence of outliers in the variables.

561 6) Although the BDC variable selection approach requires more effort than that of E-RF99,
562 with the exception of the Port Hedland site it produced either higher hit rates or
563 simultaneously higher hit rates and lower false alarm ratios for dry lightning than that of
564 E-RF99. It also tended to produce lower Brier (1950) scores and higher AUCs for LR
565 models.

566 Although a number of previous studies have examined lightning and thunderstorm activity
567 at the spatial and temporal scales of current reanalyses and GCMs, very few of these studies
568 have considered 'dry' and 'wet' systems separately. The results presented here are intended
569 to lead to an improved ability to classify deep convective systems in terms of their likelihood
570 of being 'dry' or 'wet', as well as enhanced capability to understand the observed

571 climatological characteristics of these systems. It is envisaged that the approach of this study
572 will find application in future studies involving finer-scale reanalyses and GCM runs as they
573 become available. Such work might lead to classification decision rules and boundaries that
574 are less dependent on model parameterizations. Given the importance of dry thunderstorms
575 for the ignition of wildfires by lightning, as well as wet thunderstorms in relation to a range
576 of associated hazards (including extreme rainfall), a greater understanding of dry and wet
577 thunderstorms could have significant benefits for improved resilience to the impacts of
578 lightning and thunderstorms throughout the world.

579

580 *Acknowledgments.* The CIGRE 500 lightning flash counter registration data were
581 provided by the Observations and Engineering Branch, Australian Bureau of Meteorology.
582 Financial support for this work was provided by the Australian Climate Change Science
583 Program, administered by the Department of Environment. We are indebted to Lorraine Bates
584 for her assistance with data checking and coding. All data used in this work are available on
585 request from Andrew J. Dowdy (andrew.dowdy@bom.gov.au). We also thank three
586 anonymous referees and the Editor of this journal, Andrew Ellis, for their thoughtful and
587 constructive comments on the original manuscript.

588

589 APPENDIX

590 Representation of atmospheric variables

591 Most of the daily atmospheric variable information is available at single pressure level or
592 is defined as a mean or difference for fixed pressure levels and hence can be considered as a
593 function of two spatial dimensions: $z = f(x, y)$. An exception is convective mass flux (CMF)
594 which, by definition, has a constant value across all 49 grid points for a given day and UTC
595 time. Other variables such as air temperature, minimum geostrophic vorticity, vertical

596 velocity, specific humidity, and zonal and meridional wind are defined for specific
 597 atmospheric pressure levels (p) at each grid point (Table 2). These variables can be
 598 considered as a function of three spatial dimensions: $z = f(x, y, p)$. For each day, quadratic
 599 surfaces were fitted to the atmospheric fields for 0600 UTC using ordinary least squares. A
 600 quadratic surface in two spatial dimensions is defined by

601

$$602 \quad z = f(x, y) = c_1 + c_2x + c_3x^2 + c_4y + c_5xy + c_6y^2 \quad (\text{A.1})$$

603

604 and the corresponding surface in three spatial dimensions by

605

$$606 \quad z = f(x, y, p) = c_1 + c_2x + c_3x^2 + c_4y + c_5xy + c_6y^2 + c_7p +$$

$$607 \quad c_8xp + c_9yp + c_{10}p^2 \quad (\text{A.2})$$

608

609 Instead of fitting (A.1) and (A.2) directly, the linear and quadratic terms were replaced by
 610 orthogonal polynomials in order to ensure that: the intercept and linear and quadratic
 611 regression coefficients are independent of each other (i.e. they do not change when higher-
 612 order terms are added); the estimates of the intercept and regression coefficients are placed on
 613 the same scale; and it allows the decomposition of relationships into general components of
 614 magnitude as well as into linear and nonlinear rates of change. The estimates were calculated
 615 in a coordinate system centered on the CIGRE 500 sensor (i.e., a 7×7 grid described in
 616 Section 2a). The adjusted R^2 was used as a goodness-of-fit measure for the quadratic surfaces.

617 Let $\theta_1, \dots, \theta_{10}$ denote the orthogonal polynomial regression coefficients. Five low-
 618 dimensional summary statistics (LDSS) for the above surfaces were used to facilitate physical
 619 interpretation: the intercept which is equivalent to the mean across the domain ($\mu = \theta_1$); the

620 magnitude of the gradient vector (gd) and its direction (dr) in the $x - y$ plane; Gaussian
 621 curvature (gc); and vertical gradient ($vg = c_7$). The magnitude of the gradient vector and its
 622 direction in terms of linear rate of change are defined by $gd = \sqrt{\theta_2^2 + \theta_4^2}$ and $dr = \tan^{-1}(\theta_4/\theta_2)$
 623 . Given the use of orthogonal polynomial regression, the values of gd and dr are the same as
 624 those that would have been obtained had a linear surface been fitted to the data. Gaussian
 625 curvature is an intrinsic geometric property of a surface which is independent of the
 626 coordinate system used to describe it. It is defined by

627

$$628 \quad gc = \det(\mathbf{H}) = \lambda_1 \lambda_2 \quad (\text{A.3})$$

629

630 where $\det(\bullet)$ denotes the determinant, \mathbf{H} is the Hessian matrix given by

631

$$632 \quad \mathbf{H} = \begin{bmatrix} \frac{\partial^2 z}{\partial x^2} & \frac{\partial^2 z}{\partial x \partial y} \\ \frac{\partial^2 z}{\partial y \partial x} & \frac{\partial^2 z}{\partial y^2} \end{bmatrix} = \begin{bmatrix} 2\theta_3 & \theta_5 \\ \theta_5 & 2\theta_6 \end{bmatrix} \quad (\text{A.4})$$

633

634 and λ_1 and λ_2 are the eigenvalues of \mathbf{H} (also the maximum and minimum principal

635 curvatures).

636

637

REFERENCES

638

639 Abalos, M., B. Legras, F. Ploeger, and W. J. Randel, 2015: Evaluating the advective Brewer-
 640 Dobson circulation in three reanalyses for the period 1979-2012. *J. Geophys. Res. Atmos.*,
 641 **120**, 7534-7554, doi:10.1002/2015JD023182.

642

643 Abatzoglou, J. T., C. A. Kolden, J. K. Balch, and B. A. Bradley, 2016: Controls on
644 interannual variability in lightning-caused fire activity in the western US. *Environ. Res. Lett.*,
645 **11**, 1-11, doi:10.1088/1748-9326/11/4/045005.

646

647 Alfons, A., 2012: cvTools: Cross-validation tools for regression models. R package version
648 0.3.2. <http://CRAN.R-project.org/package=cvTools>.

649

650 Allen, J. T., D. J. Karoly, and G. A. Mills, 2011: A severe thunderstorm climatology for
651 Australia and associated thunderstorm environments. . *Aust. Meteorol. Oceanogr. J.*, **61**, 143-
652 158.

653

654 Barthe, C., W. Deierling, and M. C. Barth, 2010: Estimation of total lightning from various
655 storm parameters: A cloud-resolving study. *J. Geophys. Res.*, **115**, D24202,
656 doi:10.1029/2010JD014405.

657

658 Bates, B. C., R. E. Chandler, and A. J. Dowdy, 2015: Estimating trends and seasonality in
659 Australian monthly lightning flash counts. *J. Geophys. Res. Atmos.*, **120**, 3973–3983,
660 doi:10.1002/2014JD023011.

661

662 Belsley, D., E. Kuh, and R. Welsch, 1980: *Regression Diagnostics Identifying Influential*
663 *Data and Sources of Collinearity*. Wiley, 292 pp.

664

- 665 Blouin, K. D., M. D. Flannigan, X. Wang, and B. Kochtubajda, 2016: Ensemble lightning
666 prediction models for the province of Alberta, Canada. *Intl. J. Wildland Fire*, **25**, 421-432,
667 <http://dx.doi.org/10.1071/WF15111>.
- 668
- 669 Breiman, L., 2001: Random forests. *Mach. Learn.*, **45**, 5-32, doi:10.1023/A:1010933404324.
- 670
- 671 Brier, G. W., 1950: Verification of forecasts expressed in terms of probability. *Mon. Wea.*
672 *Rev.*, **78**, 1-3, doi: [http://dx.doi.org/10.1175/1520-0493\(1950\)078<0001:VOFEIT>2.0.CO;2](http://dx.doi.org/10.1175/1520-0493(1950)078<0001:VOFEIT>2.0.CO;2).
- 673
- 674 Burrows, W. R., C. Price, and L. J. Wilson, 2005: Warm season lightning probability
675 prediction for Canada and the northern United States. *Wea. Forecasting*, **20**, 971-988.
- 676
- 677 Chandler, R. E., 2005: On the use of generalized linear models for interpreting climate
678 variability. *Environmetrics*, **16**, 699-715, doi:10.1002/env.731.
- 679
- 680 Christian, H. J., R. J. Blakeslee, D. J. Boccippio, W. L. Boeck, D. E. Buechler, K. T. Driscoll,
681 S. J. Goodman, J. M. Hall, W. J. Koshak, D. M. Mach, and M. F. Stewart, 2003: Global
682 frequency and distribution of lightning as observed from space by the Optical Transient
683 Detector. *Journal of Geophysical Research: Atmospheres*, 108(D1).
- 684
- 685 Chronis T. G., S. J. Goodman, D. Cecil, D. Buechler, F. J. Robertson, J. Pittman, and R. J.
686 Blakeslee, 2008: Global lightning activity from the ENSO perspective. *Geophys. Res. Lett.*,
687 **35**, L19804, doi: (2008).10.1029/2008GL034321.
- 688

- 689 Dai, J., Y. Wang, L. Chen, L. Tao, J. Gu, J. Wang, X. Xu, H. Lin, and Y. Gu, 2009: A
690 comparison of lightning activity and convective indices over some monsoon-prone areas of
691 China. *Atmos. Res.*, **91**, 438-452, doi:10.1016/j.atmosres.2008.08.002.
- 692
- 693 Davies, L., C. Jakob, P. May, V. V. Kumar, and S. Xie, 2013: Relationships between the
694 large-scale atmosphere and the small-scale convective state for Darwin, Australia. *J.*
695 *Geophys. Res. Atmos.*, **118**, 11,534-11,545, doi:10.1002/jgrd.50645.
- 696
- 697 Dee, D. P., and Coauthors, 2011: The ERA-Interim reanalysis: configuration and
698 performance of the data assimilation system. *Q. J. R. Meteorol. Soc.*, **137**, 553-597,
699 doi:10.1002/qj.828.
- 700
- 701 Deierling, W., W. A. Petersen, J. Latham, S. Ellis, and H. J. Christian, 2008: The relationship
702 between lightning activity and ice fluxes in thunderstorms. *J. Geophys. Res.*, **113**, D15210,
703 doi:10.1029/2007JD009700.
- 704
- 705 Dowdy, A. J., 2015: Large-scale modelling of environments favourable for dry lightning
706 occurrence. *MODSIM2015, 21st International Congress on Modelling and Simulation.*
707 *Modelling and Simulation Society of Australia and New Zealand*, Gold Coast, Queensland,
708 Australia, T. Weber, M. J. McPhee, and R. S. Anderssen, Eds, 1524-1530, ISBN: 978-0-
709 9872143-5-5. [Available online at www.mssanz.org.au/modsim2015/G4/dowdy.pdf.]
- 710
- 711 Dowdy, A. J., 2016: Seasonal forecasting of lightning and thunderstorm activity in tropical
712 and temperate regions of the world. *Sci. Rep.*, **6**, doi:10.1038/srep20874.
- 713

- 714 Dowdy, A. J., and Y. Kuleshov, 2014: Lightning climatology of Australia: temporal and
715 spatial variability. *Aust. Meteorol. Oceanogr. J.*, **64**, 103-108.
716
- 717 Dowdy, A. J., and G. A. Mills, 2009: Atmospheric States Associated with the Ignition of
718 Lightning-Attributed Fires. CAWCR Tech. Rep. No. 019, 34 pp.
719
- 720 Dowdy, A. J., and G. A. Mills, 2012a: Characteristics of lightning-attributed fires in south-
721 east Australia. *Int. J. Wildland Fire*, **21**, 521–524, doi.org/10.1071/WF10145.
722
- 723 Dowdy, A. J., and G. A. Mills, 2012b: Atmospheric and fuel moisture characteristics
724 associated with lightning-attributed fires. *J. Appl. Meteor. Climatol.*, **51**, 2025-2037,
725 doi:10.1175/JAMC-D-11-0219.1.
726
- 727 Ensor, L. A., and Robeson, S. M., 2008: Statistical characteristics of daily precipitation:
728 Comparisons of gridded and point datasets. *J. Appl. Meteor. Climatol.*, **47**, 2468-2476,
729 doi:10.1175/2008JAMC1757.1.
730
- 731 Everitt, B. S., and G. Dunn, 2001: *Applied Multivariate Data Analysis*. Second edition.
732 Arnold, 342 pp.
733
- 734 Everitt, B., and T. Hothorn, 2011: *An Introduction to Applied Multivariate Analysis with R*.
735 Springer, 273 pp.
736
- 737 Faraway, J. J., 2016: *Extending the linear model with R: generalized linear, mixed effects and*
738 *nonparametric regression models*. Second edition. Chapman and Hall / CRC Press, 399 pp.

739

740 Goodman S. J., D. E. Buechler, K. Knupp, D. Driscoll, and E. E. McCaul Jr., 2000: The
741 1997–98 El Niño event and related wintertime lightning variations in the southeastern United
742 States. *Geophys. Res. Lett.* **27**, 541–544, doi:10.1029/1999GL010808.

743

744 Hendrickx, J., 2012: perturb: Tools for evaluating collinearity. R package version 2.05.
745 <http://CRAN.R-project.org/package=perturb>.

746

747 Hilbe, J. M., 2009: *Logistic regression models*. Chapman and Hall/CRC, 656 pp.

748

749 Jayaratne, E. R., and Y. Kuleshov, 2006: Geographical and seasonal characteristics of the
750 relationship between lightning ground flash density and rainfall within the continent of
751 Australia. *Atmos. Res.*, **79**, 1–14, doi:10.1016/j.atmosres.2005.03.004.

752

753 Kasischke, E. R., T. S. Rupp, and D. L. Verbyla, 2006: Fire trends in the Alaskan Boreal
754 Forest. *Alaska's Changing Boreal Forest*, F. S. Chapin, M. Oswood, K. van Cleve, L.
755 Viereck, and D. Verbyla, Eds., Oxford University Press, 285-301.

756

757 Kuleshov, Y., and E. R. Jayaratne, 2004: Estimates of lightning ground flash density in
758 Australia and its relationship to thunder-days. *Aust. Meteorol. Mag.*, **53**, 189–196.

759

760 Kuleshov, Y., D. Mackerras, and M. Darveniza, 2009: Spatial distribution and frequency of
761 thunderstorms and lightning in Australia. *Lightning: Principles, Instruments and*
762 *Applications*, H. D. Betz, U. Schumann, and P. Laroche, Eds., Springer, 187–207,
763 doi:10.1007/978-1-4020-9079-0_8.

764

765 Kuo, H. L., and W. H. Raymond, 1980: A quasi-one-dimensional cumulus cloud model and
766 parametrization of cumulus heating and mixing effects. *Mon. Wea. Rev.*, **108**, 991–1009, doi:
767 [http://dx.doi.org/10.1175/1520-0493\(1980\)108<0991:AQODCC>2.0.CO;2](http://dx.doi.org/10.1175/1520-0493(1980)108<0991:AQODCC>2.0.CO;2).

768

769 Lang, T. J., S. A. Rutledge, B. Dolan, P. Krehbiel, W. Rison, and D. T. Lindsey, 2014:
770 Lightning in wildfire smoke plumes observed in Colorado during summer 2012. *Mon. Wea.*
771 *Rev.*, **142**, 489-507, doi:<http://dx.doi.org/10.1175/MWR-D-13-00184.1>.

772

773 Liaw, A., and M. Wiener, 2002: Classification and Regression by randomForest. *R News*, **2**,
774 18-22.

775

776 Luke, R. H., and A. G. McArthur, 1978: *Bushfires in Australia*. Australian Government
777 Publishing Service, 368 pp.

778

779 Magi, B. I., 2015: Global lightning parameterization from CMIP5 climate model output. *J.*
780 *Atmos. Oceanic Technol.*, **32**, 434-452, doi:10.1175/JTECH-D-13-00261.1.

781

782 McRae, R. H. D., 1992: Prediction of areas prone to lightning ignition. *Intl. J. Wildland Fire*,
783 **2**, 123-130, doi:10.1071/WF9920123.

784

785 Morris, J. S., 2015: Functional regression. *Annu. Rev. Stat. Appl.*, **2**, 321-359,
786 doi:10.1146/annurev-statistics-010814-020413.

787

- 788 Muñoz, Á. G., J. Díaz-Lobato, X. Chourio, and M. J. Stock, 2016: Seasonal prediction of
789 lightning activity in North Western Venezuela: Large-scale versus local drivers. *Atmos. Res.*,
790 **172-173**, 147-162, doi:10.1016/j.atmosres.2015.12.018
791
- 792 Nauslar, N. J., M. L. Kaplan, J. Wallmann, and T. J. Brown, 2013: A forecast procedure for
793 dry thunderstorms. *J. Oper. Meteor.*, **1**, 200-214,
794 doi:<http://dx.doi.org/10.15191/nwajom.2013.0117>.
795
- 796 NCAR - Research Applications Laboratory, 2015: verification: Weather Forecast Verification
797 Utilities. R package version 1.42. <http://CRAN.R-project.org/package=verification>.
798
- 799 R Core Team (2015). R: A language and environment for statistical computing. R Foundation
800 for Statistical Computing, Vienna, Austria. URL <http://www.R-project.org/>.
801
- 802 Rakov, V. A. and M. A. Uman, 2003: *Lightning: Physics and Effects*, Cambridge University
803 Press, 687 pp.
804
- 805 Ripley, B., 2014: tree: Classification and regression trees. R package version 1.0-35.
806 <http://CRAN.R-project.org/package=tree>.
807
- 808 Romero, R., M. Gayà, and C. A. Doswell, 2007: European climatology of severe convective
809 storm environmental parameters: A test for significant tornado events. *Atmos. Res.*, **83**, 389-
810 404, doi:10.1016/j.atmosres.2005.06.011.
811

- 812 Romps, D. M., J. T. Seeley, D. Vollaro, and J. Molinari, 2014: Projected increase in lightning
813 strikes in the United States due to global warming. *Science*, **346**, 851-854,
814 doi:10.1126/science.1259100.
- 815
- 816 Rorig, M. L., and S. A. Ferguson, 1999: Characteristics of lightning and wildland fire ignition
817 in the Pacific Northwest. *J. Appl. Meteor.*, **38**, 1565-1575,
818 doi:http://dx.doi.org/10.1175/1520-0450(1999)038<1565:COLAWF>2.0.CO;2.
- 819
- 820 Rorig, M. L., S. J. McKay, S. A. Ferguson, and P. Werth, 2007: Model-generated predictions
821 of dry thunderstorm potential. *J. Appl. Meteor. Climatol.*, **46**, 605-614,
822 doi:http://dx.doi.org/10.1175/JAM2482.1.
- 823
- 824 Rothermel, R. C., 1972: A mathematical model for predicting fire spreads in wildland fuels.
825 U.S. Forest Service Res. Paper INT-115, 40 pp.
- 826
- 827 Sanchez, G., 2013: DiscriMiner: Tools of the Trade for Discriminant Analysis. R package
828 version 0.1-29. <http://CRAN.R-project.org/package=DiscriMiner>.
- 829
- 830 Takahashi, T., and K. Miyawaki, 2002: Reexamination of riming electrification in a wind
831 tunnel. *J. Atmos. Sci.*, **59**, 1018-1025, doi: [http://dx.doi.org/10.1175/1520-](http://dx.doi.org/10.1175/1520-0469(2002)059<1018:ROREIA>2.0.CO;2)
832 [0469\(2002\)059<1018:ROREIA>2.0.CO;2](http://dx.doi.org/10.1175/1520-0469(2002)059<1018:ROREIA>2.0.CO;2).
- 833
- 834 Tiedtke, M., 1989: A comprehensive mass flux scheme for cumulus parameterization in
835 large-scale models. *Mon. Wea. Rev.*, **117**, 1779–1800, doi:http://dx.doi.org/10.1175/1520-
836 [0493\(1989\)117<1779:ACMFSF>2.0.CO;2](http://dx.doi.org/10.1175/1520-0493(1989)117<1779:ACMFSF>2.0.CO;2).

837

838 USDA Forest Service, 1992: 1984-1990 Wildfire Statistics. State and Private Forestry, Fire
839 and Aviation Management Staff, USDA Forest Service (Washington, DC), 240 pp.

840

841 Vazquez A., and J. M. Moreno, 1998: Patterns of lightning- and people-caused fires in
842 peninsula Spain. *Intl. J. Wildland Fire*, **8**, 103-115, doi:10.1071/WF9980103.

843

844 Venables, W. N. and B. D. Ripley, 2002: *Modern Applied Statistics with S*. Fourth Edition.
845 Springer, 495 pp.

846

847 Wallmann, J., R. Milne, C. Smallcomb, and M. Mehle, 2010: Using the 21 June 2008
848 California lightning outbreak to improve dry lightning forecast procedures. *Wea.*
849 *Forecasting*, **25**, 1447-1462, doi:http://dx.doi.org/10.1175/2010WAF2222393.1.

850

851 Weisman, M. L., and J. B. Klemp, 1982: The dependence of numerically simulated
852 convective storms on vertical wind shear and buoyancy. *Mon. Wea. Rev.*, **110**, 504-520,
853 doi:http://dx.doi.org/10.1175/1520-0493(1982)110<0504:TDONSC>2.0.CO;2.

854

855 Williams, E., V. Mushtak, D. Rosenfeld, S. Goodman, and D. Boccippio, 2005:
856 Thermodynamic conditions favorable to superlative thunderstorm updraft, mixed phase
857 microphysics and lightning flash rate. *Atmos. Res.*, **76**, 288-306,
858 doi:10.1016/j.atmosres.2004.11.009.

859

860 Wotton B. M., and D. L. Martell, 2005: A lightning fire occurrence model for Ontario. *Can.*
861 *J. For. Res.*, **35**, 1389-1401, doi:10.1139/x05-071.

862

863 Wotton, B. M., B. J. Stocks, and D. L. Martell, 2005: An index for tracking sheltered forest
864 floor moisture within the Canadian Forest Fire Weather Index System. *Intl. J. Wildland Fire*,
865 **14**, 169-182, <http://dx.doi.org/10.1071/WF04038>.

866

867 Xu, W., E. J. Zipser, C. Liu, and H. Jiang, 2010: On the relationship between lightning
868 frequency and thundercloud parameters of regional precipitation systems. *J. Geophys. Res.*,
869 *Atmos.*, **115**, D12203, doi:10.1029/2009JD013385.

870

871 Yan, Z., S. Bate, R. E. Chandler, V. Isham, and H. S. Wheater, 2002: An analysis of daily
872 maximum windspeed in northwestern Europe using generalized linear models. *J. Climate*, **15**,
873 2073-2088, doi:[http://dx.doi.org/10.1175/1520-0442\(2002\)015<2073:AAODMW>2.0.CO;2](http://dx.doi.org/10.1175/1520-0442(2002)015<2073:AAODMW>2.0.CO;2).

874

875 Youden, W. J., 1950: Index for rating diagnostic tests. *Cancer* **3**, 32–35, doi:10.1002/1097-
876 0142(1950)3:1<32::AID-CNCR2820030106>3.0.CO;2-3.

877

878

879

880

881 TABLE 1. Site and data details for CIGRE 500 lightning flash counters. Daily lightning flash count records cover the period from January 2004

882

to at least December 2010 (Townsville) and at most February 2013 (Melbourne).

Site		Altitude		No. of lightning	Proportion dry	Proportion wet
No.	Location	(m)	Köppen classification	days	lightning days	lightning days
1	Darwin	30	Tropical savanna climate (Aw)	1350	0.53	0.47
2	Townsville	4	Tropical savanna climate (Aw)	286	0.53	0.47
3	Coffs Harbour	5	Humid subtropical climate (Cfa)	501	0.58	0.42
4	Melbourne	113	Marine west coast (Cfb)	570	0.64	0.36
5	Perth	15	Mediterranean (Csa)	148	0.55	0.45
6	Port Hedland	6	Subtropical desert (BWh)	401	0.81	0.19

883

884

885

886

887

TABLE 2. Abbreviations, full names, units of measure and specifications for atmospheric variables.

Abbreviation	Full name	Specification
<i>Instability and lifting potential</i>		
CAPE	Convective available potential energy (J kg^{-1})	As provided in ERA-Interim reanalysis (maximum CAPE based on lifting parcels within a near-surface layer)
CBH	Cloud base height (m)	Based on temperature and dewpoint at a height of 2 m with lifting to condensation level using an idealized constant lapse rate
CMF	Convective mass flux ($\text{Pa}^2 \text{s}^{-1} \text{K}^{-1}$)	500 hPa: calculated as the product of air density, fraction of grid points covered by updrafts within the 7x7 gridded region, and the vertical velocity averaged across all updrafts.

CONV1000850	Mean low-level horizontal wind convergence (s^{-1})	Mean value at 850 and 1000 hPa pressure levels
DD	Dewpoint depression ($^{\circ}C$)	500, 700 and 850 hPa
DDIV	Density-weighted mean upper-level divergence minus density-weighted mean low-level divergence (s^{-1})	{300, 400} – {850, 1000} hPa
EPTL	Mean low-level equivalent potential temperature minus mean mid-level equivalent potential temperature ($^{\circ}C$)	Mean value at 1000 and 850 hPa – mean value at 700 and 500 hPa
TD850T500	Cross totals index ($^{\circ}C$)	850 and 500 hPa
TGD	Direction of thickness gradient (rad)	{500, 700}, {500, 1000} and {700, 1000} hPa
TGM	Magnitude of thickness gradient ($m^2 s^{-2}$)	{500, 700}, {500, 1000} and {700, 1000} hPa
THETA_W1000	Wet-bulb potential temperature ($^{\circ}C$)	1000 hPa
THETA_W850500	Wet-bulb potential temperature difference ($^{\circ}C$)	850 – 500 hPa
THK7001000	Geopotential thickness ($m^2 s^{-2}$)	700 – 1000 hPa geopotential heights
TL850500	Temperature lapse ($^{\circ}C$)	850 – 500 hPa

TL850700	Temperature lapse ($^{\circ}\text{C}$)	850 – 700 hPa
TTI	Total totals index ($^{\circ}\text{C}$)	850 and 500 hPa
W	Vertical velocity (Pa s^{-1})	200, 300, 500, 700, 850 and 1000 hPa
<i>Atmospheric water content</i>		
CONVP	Convective precipitation (m)	As provided in ERA-Interim reanalysis
ICE	Total column ice water (kg m^{-2})	As provided in ERA-Interim reanalysis
SH	Specific humidity (kg kg^{-1})	500, 700 and 850 hPa
TCWV	Total column water vapor (kg m^{-2})	As provided in ERA-Interim reanalysis
TOTP	Total precipitation (m)	As provided in ERA-Interim reanalysis
<i>Wind speed</i>		
MVWS	Maximum vertical wind shear (m s^{-1})	300 to 850 hPa
S06	Vertical wind shear between 0 and 6 km (m s^{-1})	1000 and 500 hPa
U	Zonal wind velocity (m s^{-1})	300, 500, 700, 850 and 1000 hPa

V	Meridional wind velocity (m s^{-1})	300, 500, 700, 850 and 1000 hPa
<i>General atmospheric state and variability</i>		
SEASON	Season-of-year	DJF, MAM, JJA and SON
T	Air temperature ($^{\circ}\text{C}$)	2 meters, 500, 700 and 850 hPa
MSLP	Mean sea level pressure (Pa)	As provided in ERA-Interim reanalysis
GPH	Geopotential height ($\text{m}^2 \text{s}^{-2}$)	500 and 700 hPa
MING	Minimum geostrophic vorticity (s^{-2})	Laplacian of geopotential at 500, 700 and 850 hPa

889

890

TABLE 3. Frequently used acronyms and abbreviations

Acronym or abbreviation	Full name
AUC	Area under receiver operating characteristic curve
BDC	Approach of Bates, Dowdy and Chandler (this paper)
BS	Brier (1950) score
CART	Classification and regression trees
E-RF99	Extended approach of Rorig and Ferguson (1999)
FAR	False alarm ratio for dry lightning
GCM	General circulation model
HR	Hit rate for dry lightning
LDA	Linear discriminant analysis
LDSS	Low-dimensional summary statistics
LR	Logistic regression
QDA	Quadratic discriminant analysis
RF	Random forests
RF99	Approach of Rorig and Ferguson (1999)
ROC	Receiver operating characteristic

893 LIST OF FIGURES

894 FIG. 1. Locations of CIGRE 500 lightning flash counters (filled circles) and relative
895 proportions of dry lightning and wet lightning days in daily lightning flash count series. Key
896 to numerals is given in Table 1. Widths of gray rectangles indicate proportions of dry
897 lightning days and heights proportions of wet lightning days.

898 FIG. 2. Examples of comparative boxplots of potential candidate variables for the Coffs
899 Harbour CIGRE 500 site: (a) mu.CBH, (b) mu.CONVP, (c) mu.DD700, (d) mu.DD850, (e)
900 mu.ICE, and (f) mu.TOTP.

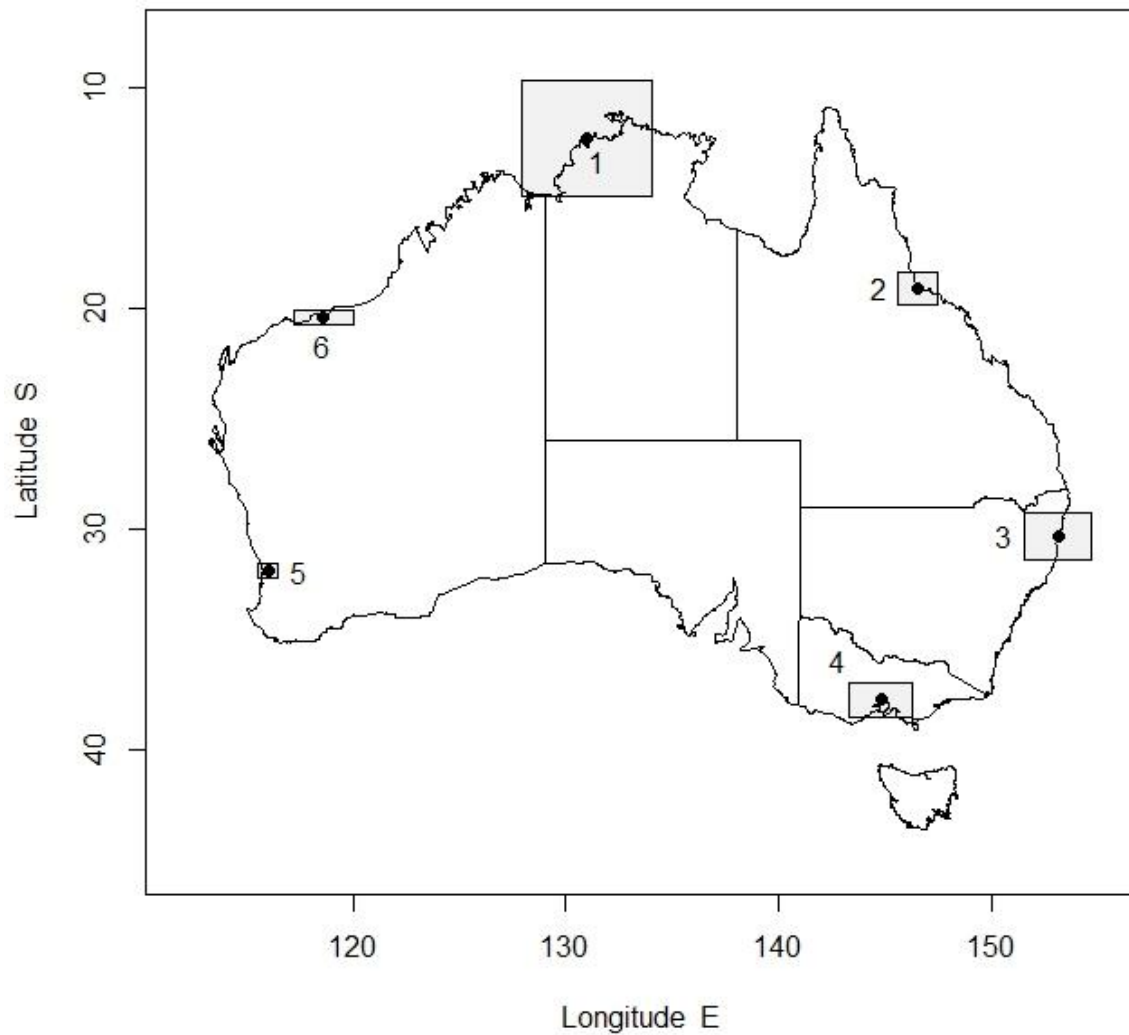
901 FIG. 3. Skill scores obtained using the methods of E-RF99 (filled squares) and BDC
902 (filled triangles) for five classifiers and six CIGRE 500 sites. Radii of the circles are
903 proportional to the Brier score. Dashed lines represent the convex hull of the false alarm ratio
904 (FAR) and hit rate (HR) values for dry lightning obtained using the methods of E-RF99.

905 FIG. 4. Relative frequency histogram of selected variables across six CIGRE 500 sites and
906 four classifiers: classification and regression trees (CART), random forests (RF), linear
907 discriminant analysis (LDA) and logistic (LR).

908 FIG. 5. Relative frequency histograms of influential variables for discriminating dry
909 lightning from wet lightning days for each CIGRE 500 site across four classifiers:
910 classification and regression trees (CART), random forests (RF), linear discriminant analysis
911 (LDA) and logistic (LR).

912 FIG. 6. Mean skill scores obtained from cross validation experiments using the methods of
913 E-RF99 (filled squares) and BDC (filled triangles) for five classifiers and six CIGRE 500
914 sites. Radii of the circles are proportional to the Brier score. Dashed lines represent the
915 convex hull of the mean false alarm ratio (FAR) and hit rate (HR) values for dry lightning
916 obtained using the methods of E-RF99.

917 FIG. 7. Scatter plot of mean area under receiver operating characteristic curve (AUC)
918 values obtained from cross-validation of logistic regression (LR) models. Key to numerals is
919 given in Table 1.
920

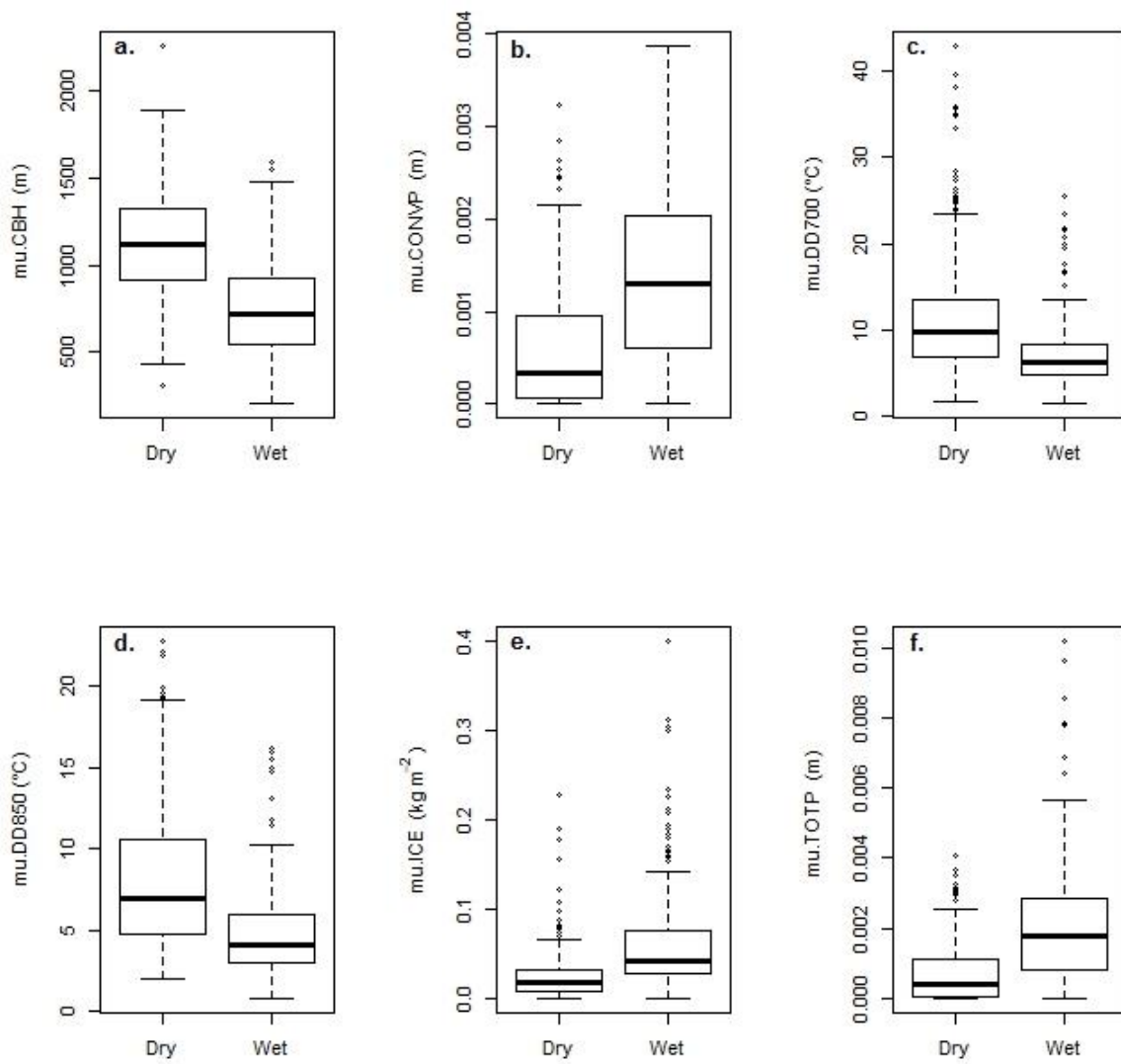


921

922

923 FIG. 1. Locations of CIGRE 500 sensors (filled circles) and relative proportions of dry
 924 lightning and wet lightning days in daily lightning flash count series. Key to numerals is
 925 given in Table 1. Widths of gray rectangles indicate proportions of dry lightning days and
 926 heights proportions of wet lightning days.

927



928

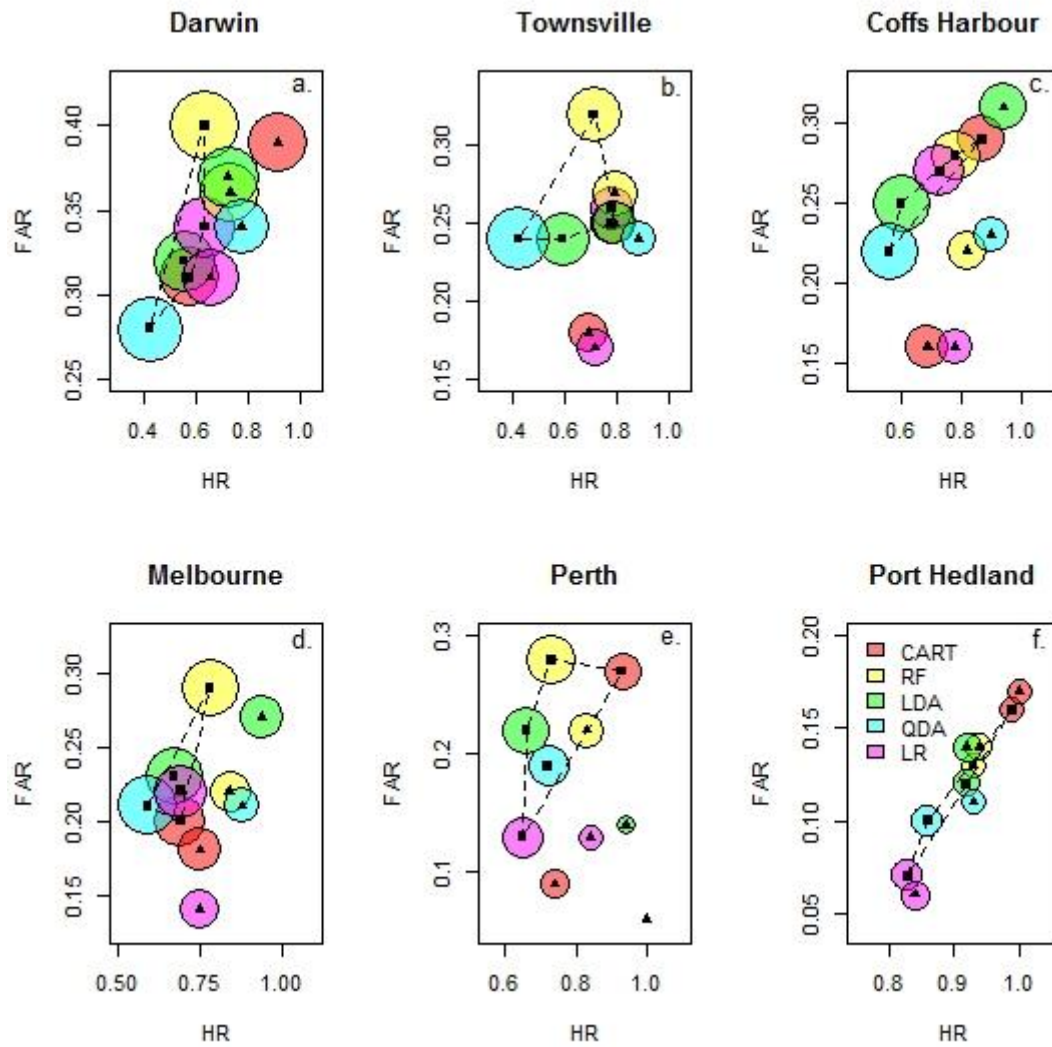
929

930 FIG. 2. Examples of comparative boxplots of potential candidate variables for the Coffs

931 Harbour CIGRE 500 site: (a) mu.CBH, (b) mu.CONVP, (c) mu.DD700, (d) mu.DD850, (e)

932 mu.ICE, and (f) mu.TOTP.

933



934

935

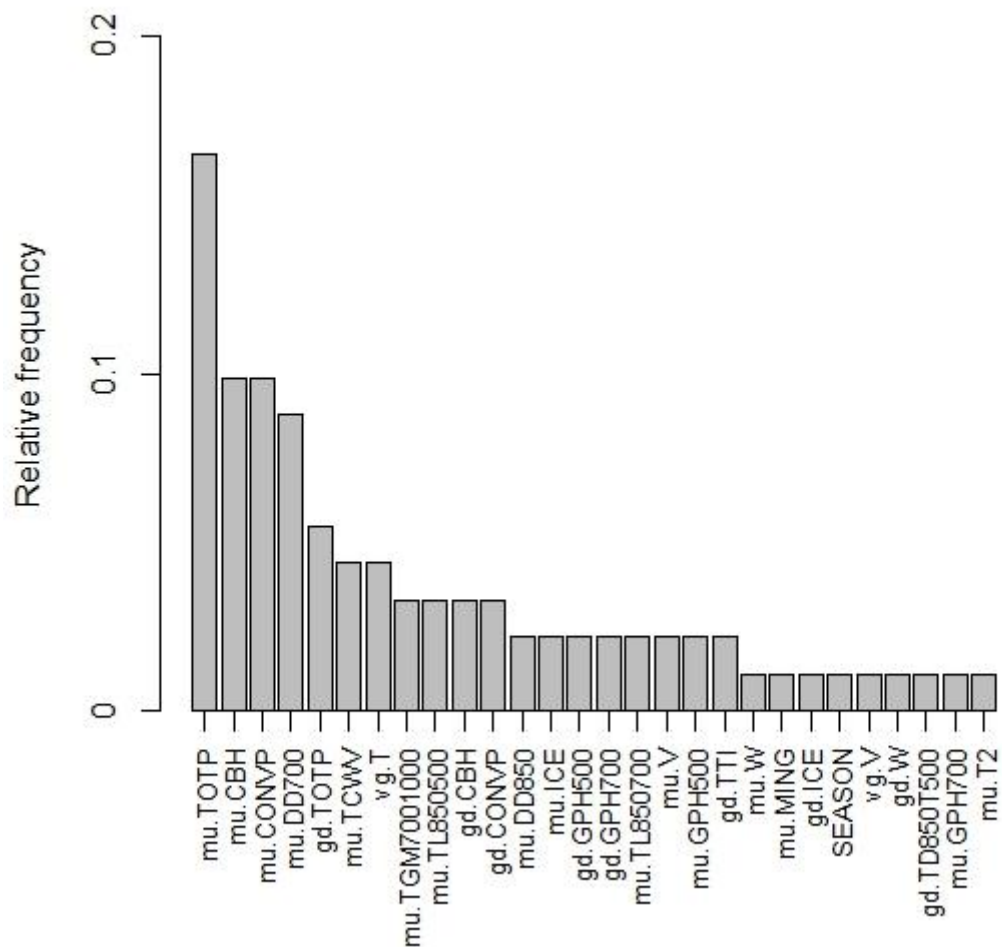
936 FIG. 3. Skill scores obtained using the methods of E-RF99 (filled squares) and BDC

937 (filled triangles) for five classifiers and six CIGRE 500 sites. Radii of the circles are

938 proportional to the Brier score. Dashed lines represent the convex hull of the false alarm ratio

939 (FAR) and hit rate (HR) values for dry lightning obtained using the methods of E-RF99.

940



941

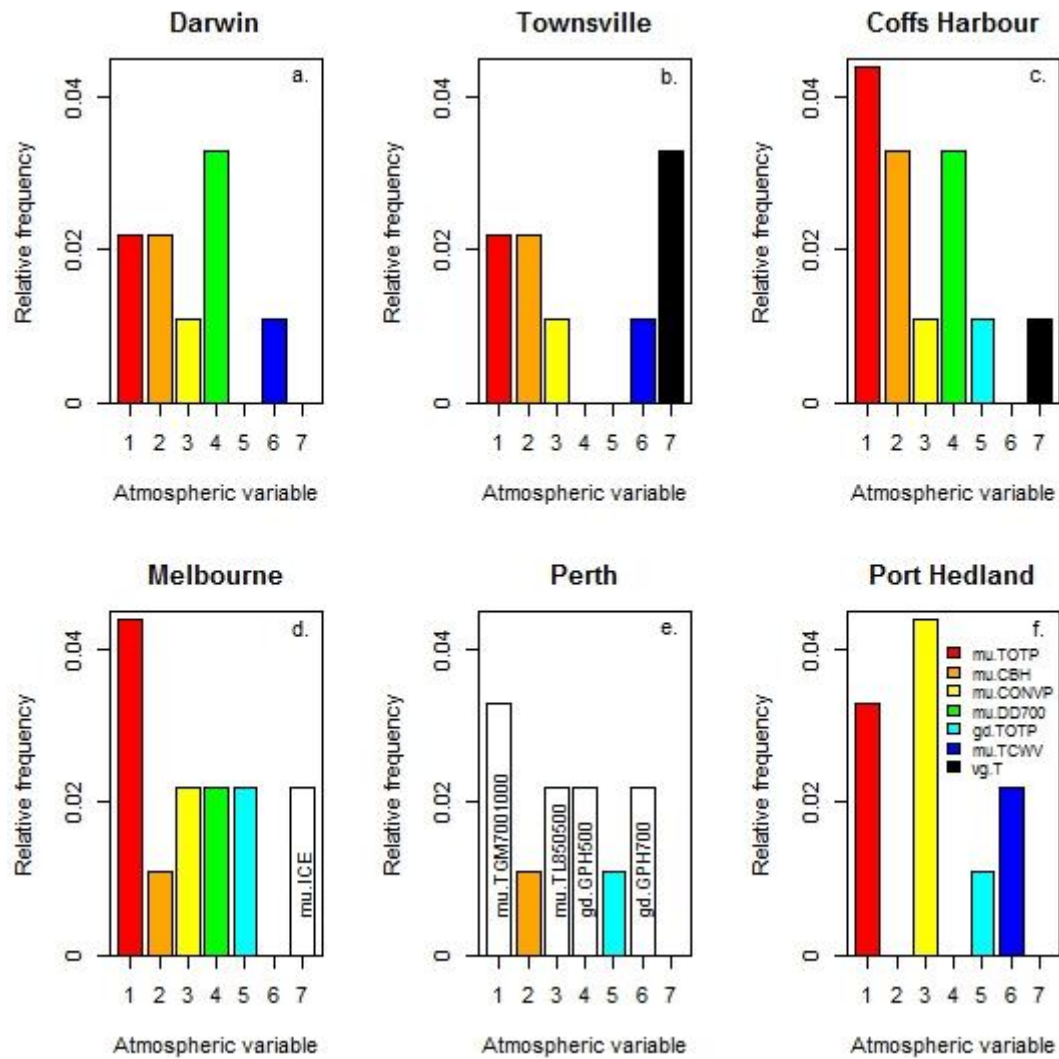
942

943 FIG. 4. Relative frequency histogram of selected variables across six CIGRE 500 sites and

944 four classifiers: classification and regression trees (CART), random forests (RF), linear

945 discriminant analysis (LDA) and logistic (LR).

946



947

948

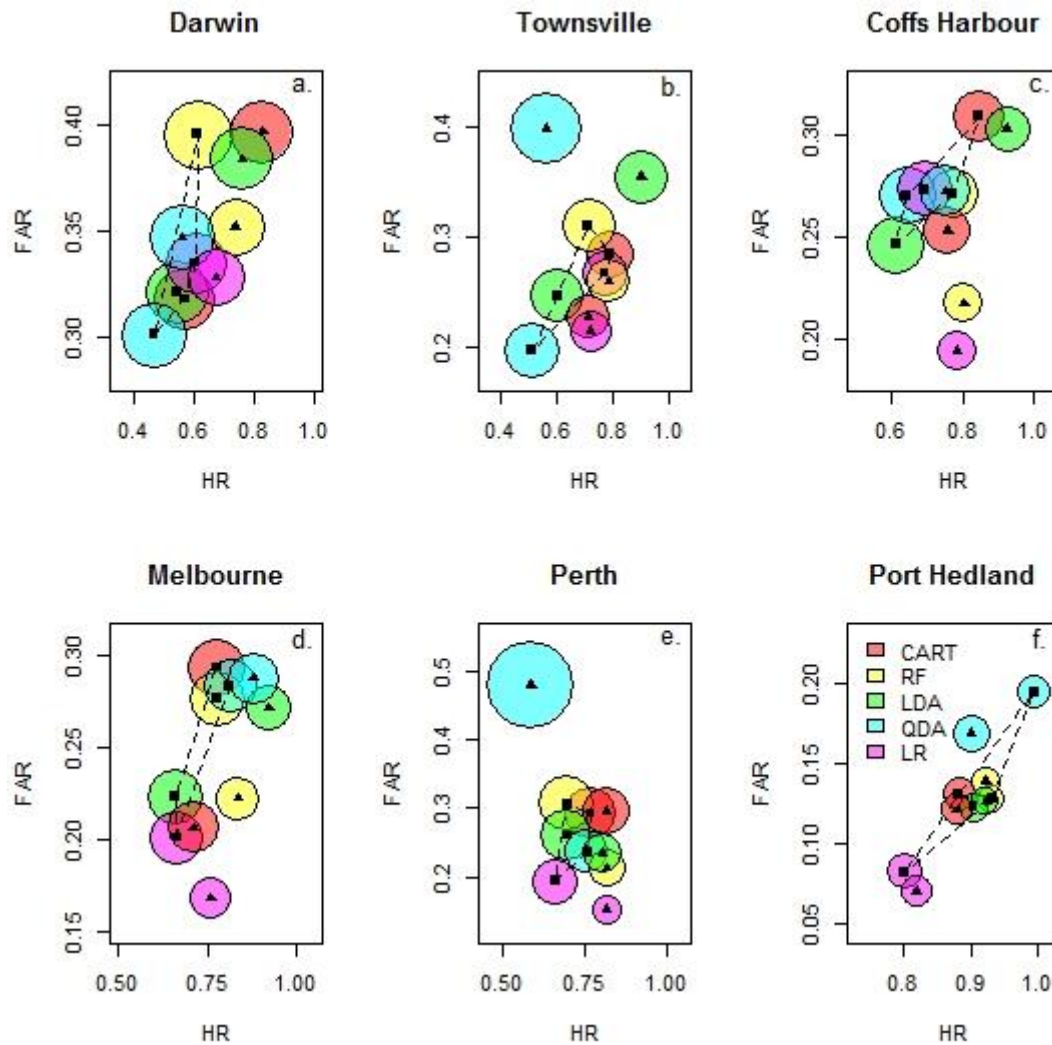
949 FIG. 5. Relative frequency histograms of influential variables for discriminating dry

950 lightning from wet lightning days for each CIGRE 500 site across four classifiers:

951 classification and regression trees (CART), random forests (RF), linear discriminant analysis

952 (LDA) and logistic (LR).

953



954

955

956 FIG. 6. Mean skill scores obtained from cross validation experiments using the methods of

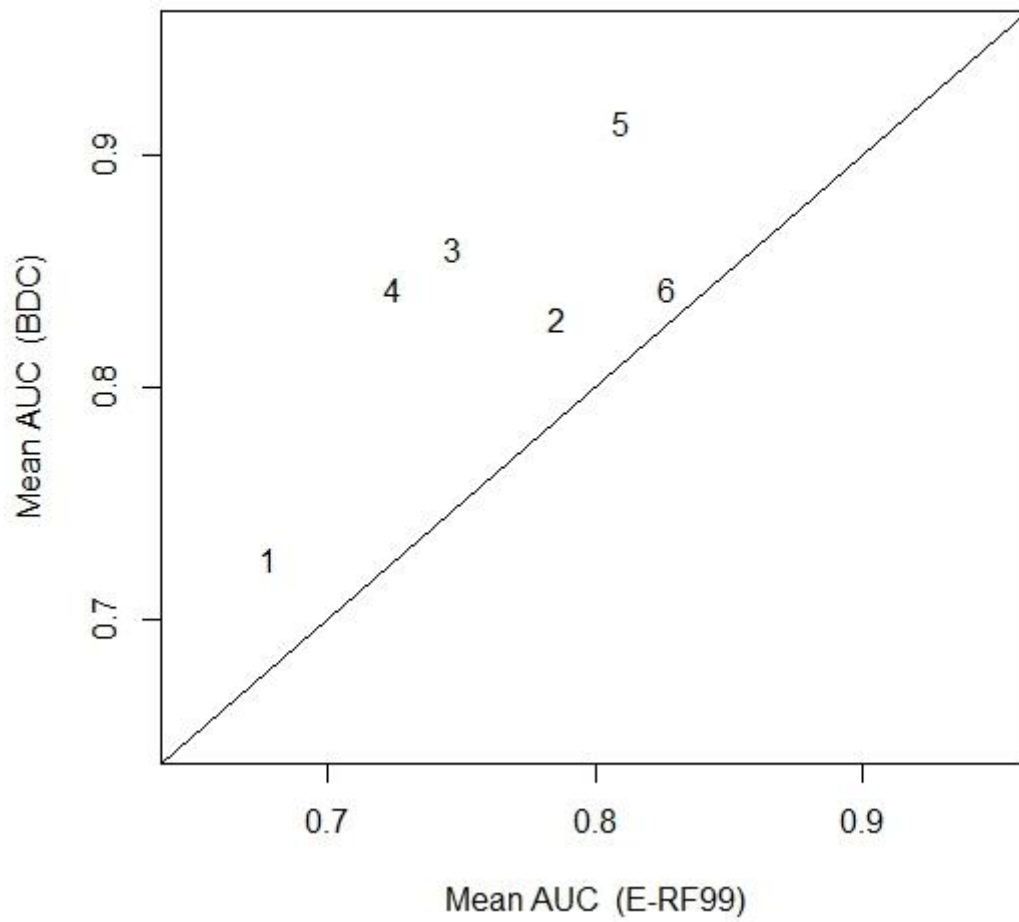
957 E-RF99 (filled squares) and BDC (filled triangles) for five classifiers and six CIGRE 500

958 sites. Radii of the circles are proportional to the Brier score. Dashed lines represent the

959 convex hull of the mean false alarm ratio (FAR) and hit rate (HR) values for dry lightning

960 obtained using the methods of E-RF99.

961



962

963

964 FIG. 7. Scatter plot of mean area under receiver operating characteristic curve (AUC)

965 values obtained from cross-validation of logistic regression (LR) models. Key to numerals is

966 given in Table 1.

967